Available online at www.sciencedirect.com

SCIENCE @ DIRECT®

Trans. Nonferrous Met. Soc. China 17(2007) 1282−1286

Transactions of
Nonferrous Metals
Society of China

www.csu.edu.cn/ysxb/

# Low temperature oxidation of Cr-alloyed $MoSi_2$

E. Ström[1], Y. Cao[2], Y. M. Yao[2]

1. Kanthal AB, Box 502, SE-734 27 Hallstahammar, Sweden;
2. Department of Materials and Manufacturing Technology, Chalmers University Technology,
SE-412 96 Gothenburg, Sweden

Received 15 July 2007; accepted 10 September 2007

**Abstract:** Cr-alloyed $MoSi_2$ was compared with monolithic $MoSi_2$ with respect to oxidation at 450 ℃ for 456 h. Phases formed on Cr-alloyed $MoSi_2$ after exposure are $Cr_2(MoO_4)_3$, $MoO_3$, and cristobalite ($SiO_2$) according to X-ray diffraction results. Monolithic $MoSi_2$ forms $MoO_3$ and mainly amorphous $SiO_2$. X-ray photoelectron spectroscopy indicates that the main oxidation product on the outermost surface is $SiO_2$ for all studied samples. The samples form a relatively loose oxide but the oxide adherence improves with increasing Cr content. It is indicated that Cr addition can benefit pesting control in $MoSi_2$.

**Key words:** molybdenum silicides; pesting; oxidation; alloying

## 1 Introduction

Many intermetallics are under intensive investigation as high temperature materials. Of these, $MoSi_2$ is perhaps the most interesting, because of its high melting point (2 030 ℃), excellent oxidation resistance up to 1 800 ℃ in air and low density (6.27 g/cm$^3$). The oxidation resistance at high temperature is due to the formation of a viscous $SiO_2$ scale that can be self-healing if damaged. However, at 400−600 ℃ $MoSi_2$ suffers from catastrophic oxidation sometimes referred to as pesting[1].

There are several investigations that have dealt with the so-called pest oxidation in $MoSi_2$-based materials. As summarised in Ref.[2], some say that pest is not an intrinsic property in $MoSi_2$, as crack-free, hot isostatically pressed(HIPed) or single crystalline $MoSi_2$ does not pest. However, some reports that hot pressed or single crystalline $MoSi_2$ indeed suffers from pest oxidation[2]. In another study[3], silicon-rich $MoSi_2$ alloys were able to form protective $SiO_2$ even at 500 ℃ and showed no indication on disintegration. It has been reported that in $MoSi_2$-composites with additions of $Si_3N_4$, pesting has been overcome[4]. In silicides based on the $Mo_5SiB_2$-phase it is argued that B additions increase the fluidity of the silica scale and encapsulate the silicide grains, thereby preventing oxidation induced by cracking. However, studies so far have not been extended to temperatures below 600 ℃[5].

Alloying additions to $MoSi_2$ may alter its oxidation properties at low temperatures. Alloying studies so far have focused on additions of Ti, V, Cr, Zr, Nb, Ta, W, Re, and Al[6−7]. With a few exceptions, the alloying content has been on the order of 1% (molar fraction) corresponding to $(Mo_{0.97}M_{0.03})Si_2$, where M is the alloying element. YANAGIHARA et al[8] studied the pesting of Mo-Si-X (X=Al, Ta, Ti, Zr, and Y) to evaluate the third element effect. They reported that elements that have stronger affinity to oxygen than Si, e.g., Al, Ti, Zr, and Y, can prevent $MoSi_2$ from pesting. A possible effect of the elements that have stronger affinity for oxygen than Si is that they decrease the oxygen flux toward the oxide-intermetallic interface and increase the plasticity of the amorphous oxide formed in cracks[2]. So far, there has been no study on the effect of Cr on pesting of $MoSi_2$ reported in literature. Very promising results have been reported on Cr-rich silicide composites consisting of $(Cr,Mo)_3Si$ and $(Cr,Mo)_5Si_3$ that do not show any signs of pest even after 2 000 h at 500 ℃[9]. Therefore, in this work, polycrystalline, Cr-alloyed $MoSi_2$ was compared with monolithic $MoSi_2$ with respect to oxidation at 450 ℃.

---

**Foundation item:** Project supported by the Swedish Consortium for Materials Use in Energy Applications

**Corresponding author:** E. Ström; Tel: +46-220-21665; E-mail: erik.o.strom@kanthal.com

## 2 Experimental

The samples were prepared by sintering powders of designed compositions, i.e., $MoSi_2$, $(Mo_{0.90}Cr_{0.10})Si_2$ and $(Mo_{0.85}Cr_{0.15})Si_2$, in hydrogen at 1 615 ℃. Densities after sintering were 95.4%, 99.3% and 99.0 % of theoretical, respectively. Bulk chemical analysis was performed to determine the sample compositions as well as the C, O, and N contents. The results of the chemical analyses of the studied alloys are shown in Table 1. Nominal and measured compositions are listed in Table 2.

The microstructural characterisation and phase analysis of the alloys were carried out using scanning electron microscopy (SEM, LEO 1550 Gemini), energy dispersive spectrometry (EDS, Oxford) and X-ray diffraction (XRD, Bruker axs D8 ADVANCE diffractometer, Cr $K_\alpha$ radiation, 35 kV, 40 mA, secondary monochromator). Lattice parameter calculations of the Cr-alloyed samples were performed using monoclinic $ZrO_2$ as an internal standard. Subsequent density calculations were based on chemical analysis data. Oxidation tests were performed for 456 h (three weeks) in ambient air at 450 ℃, using $MoSi_2$ as reference material.

The samples subjected to oxidation were also characterized by X-ray photoelectron spectrometry(XPS) using a PHI5500 electron spectro- meter. The photoelectrons were generated with an Al $K_\alpha$ (1 486.6 eV) X-ray source. The acquisition conditions for the survey spectra (0−1 200 eV) were 93.9 eV pass energy, 45° take-off angle and 0.4 eV/step. Selected region spectra were recorded covering the Si2p, C1s and O 1s, Mo 3d and Cr 2p to estimate the surface concentration. The acquisition conditions were 23.5 eV pass energy, 45° take-off angle, 0.1 eV/step for the selected region spectra. The position of adventitious carbon (284.6 eV) was used to calibrate the peak shift.

## 3 Results and discussion

Table 2 shows the phase constitution, cell parameters and densities as calculated from XRD. It can be seen that the lattice parameters decrease with increasing Cr content, which indicates solid solution of Cr into the $MoSi_2$ crystal.

According to the results of UMAKOSHI et al[11] $MoSi_2$ can dissolve not more than 2.6% (molar fraction) Cr corresponding to the formula $(Mo_{0.92}Cr_{0.08})Si_2$, since their alloy with composition $(Mo_{0.90}Cr_{0.10})Si_2$ showed some C40 reflections in XRD. Some indications of C40 phase are also found in our work for this composition, i.e. 3.3% Cr. Interestingly, XRD indicates that Cr is completely dissolved into the $C11_b$ phase without forming hexagonal C40 phase for the alloy having 4.7% Cr additions, i.e., $(Mo_{0.85}Cr_{0.15})Si_2$, since no C40 reflections are found (see Fig.1). In SEM, $Cr_5Si_3$ grains containing high amounts of Mo are observed at grain junctions and grain boundaries in the matrix (see Fig.2). The Cr/Mo-ratios in $Cr_5Si_3$ as determined by EDS were 4.0 and 5.3 in Cr1 and Cr2, respectively, which explains their contrast being darker than that of the matrix phase.

Fig.3 shows the three studied samples after exposure at 450 ℃ in ambient air for 456 h. It can be noticed that there is a shift in colour with increasing Cr-addition. All samples have a loose oxide scale that is partly spalled during sample handling, though the adherence improves with Cr-alloying.

XRD patter indicates that the oxide products formed

**Table 1** Chemical compositions of investigated samples (mass fraction, %)

| Sample | C | Cr | Si | Al | Fe | Ti | O | N | Mo |
|---|---|---|---|---|---|---|---|---|---|
| $MoSi_2$ | 0.009 | - | 36.4 | 0.014 | 0.007 | 0.019 | 0.69 | 0.09 | Bal. |
| Cr1-$(Mo_{0.90}Cr_{0.10})Si_2$ | 0.013 | 3.5 | 38.1 | 0.039 | 0.009 | 0.047 | 0.37 | 0.014 | Bal. |
| Cr2-$(Mo_{0.85}Cr_{0.15})Si_2$ | 0.009 | 5.0 | 38.7 | 0.10 | 0.013 | 0.097 | 0.27 | 0.08 | Bal. |

**Table 2** Nominal and measured compositions of Cr-added samples (molar fraction, %)

| Sample | Mo | Cr | Si | a/nm | c/nm | X-ray density/$(g\cdot cm^{-3})$ |
|---|---|---|---|---|---|---|
| $MoSi_2$(nominal) | 33.3 | − | 66.7 | 0.320 64$^{1)}$ | 0.7847 8$^{2)}$ | 6.27$^{2)}$ |
| $MoSi_2$(measured) | 33.8 | − | 66.2 | n.d. | n.d. | n.d. |
| $(Mo_{0.90}Cr_{0.10})Si_2$(nominal) | 30 | 3.3 | 66.7 | | | |
| $(Mo_{0.90}Cr_{0.10})Si_2$(Cr1) | 29.95 | 3.31 | 66.74 | 0.319 70 | 0.782 2 | 6.14 |
| $(Mo_{0.85}Cr_{0.15})Si_2$(nominal) | 28.05 | 4.95 | 66.7 | | | |
| $(Mo_{0.85}Cr_{0.15})Si_2$(Cr2) | 28.48 | 4.67 | 66.85 | 0.319 40 | 0.781 4 | 6.08 |

n.d. means not determined; 1) From Ref.[9]; 2) JCPDS 41-0612

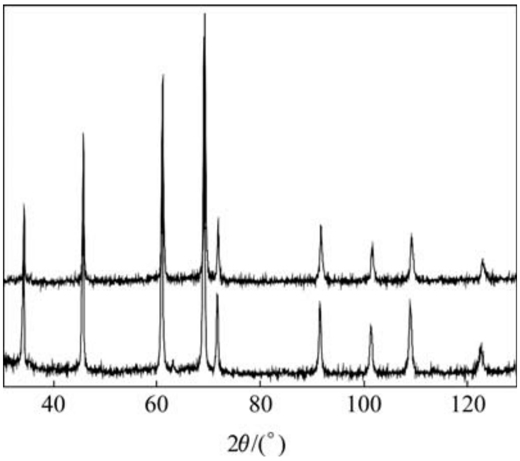

**Fig.1** XRD patterns for $(Mo_{0.90}Cr_{0.10})Si_2$ (lower) and $(Mo_{0.85}Cr_{0.15})Si_2$ (upper) (Existence of C40 phase in $(Mo_{0.90}Cr_{0.10})Si_2$ at about 63° (2$\theta$). All other reflections are from $C11_b$ phase)

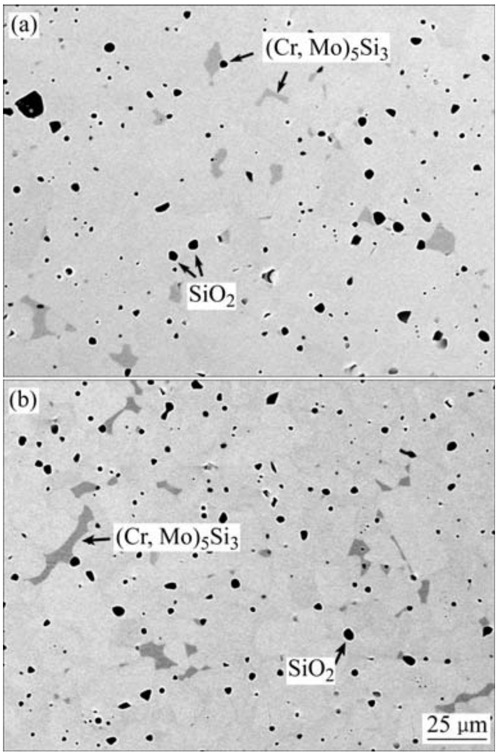

**Fig.2** Backscattered electron micrographs of sample Cr1 (a) and Cr2 (b), showing matrix phase $(Mo,Cr)Si_2$ (bright contrast) and precipitates (indicated with arrows)

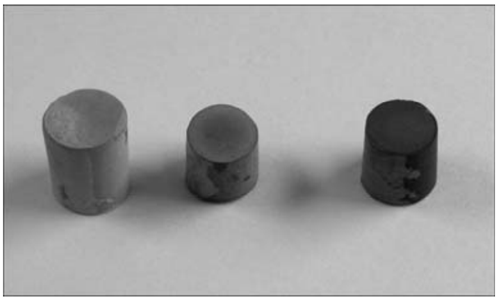

**Fig.3** Samples after exposure for 456 h in ambient air at 450 ℃ (From left to right: $MoSi_2$, Cr1, and Cr2; sample diameter about 10 mm)

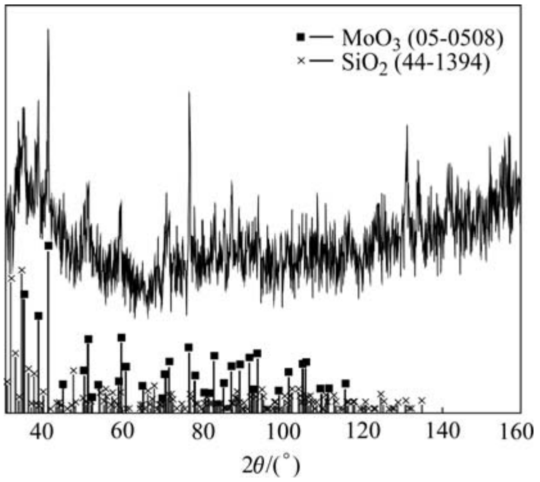

**Fig.4** XRD patterns of $MoSi_2$ after exposure at 450 ℃ in ambient air for 456 h

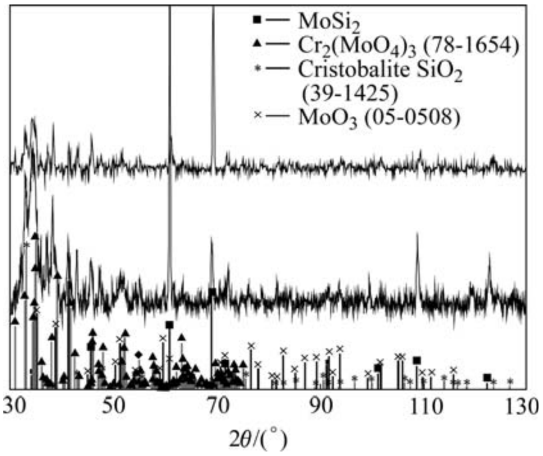

**Fig.5** XRD patterns of Cr1 (lower) and Cr2 (upper) after exposure for 456 h in ambient air at 450 ℃

on $MoSi_2$ are $MoO_3$ and $SiO_2$, though the latter seems to exist also in amorphous form due to the curvature of the background and the low acquisition rate in its diffractogram (see Fig.4). It is also indicated that the oxide is rather thick, since no reflections from the bulk are visible using normal Bragg-Brentano geometry. In contrast, reflections of the bulk are seen both for Cr1 and Cr2 despite that grazing incidence XRD is used (see Fig.5). Thus, the oxide formed on Cr1 and Cr2 is probably thinner than that formed on $MoSi_2$. The phases that were identified by XRD on Cr1 and Cr2 after exposure were $Cr_2(MoO_4)_3$, $MoO_3$, and cristobalite ($SiO_2$).

Fig.6 shows the XPS survey spectra of the samples $MoSi_2$ and Cr1 after exposure at 450 ℃ for 456 h in ambient air. It is indicated that only small amounts of Mo and/or Cr exist on the top surface, while oxygen and silicon signals are dominant. It can be seen in the inserted Si and O peaks in Fig.6 that the Si 2p has its maximum at about 103.4 eV and the O 1s has its maximum at 532.5 eV, indicating the formation of $SiO_2$. The main product on the top surface after exposure is thus $SiO_2$.

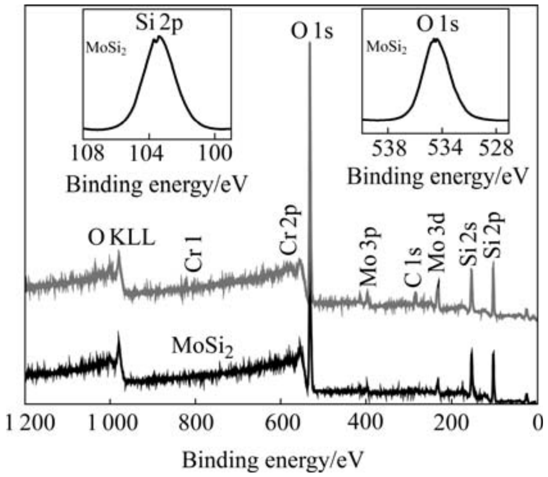

**Fig.6** XPS spectra of exposed samples $MoSi_2$ and Cr1 (Inserts are Si 2p (upper left) and O 1s (upper right) peaks)

It has been widely accepted that pesting of $MoSi_2$ is a function of temperature, microstructure, alloying element, composition, and atmosphere. For alloyed $C11_b$-$MoSi_2$, STERGIOU and TSAKIROPOULOS reported that neither Ta (C40 structure stabilizer) nor W ($C11_b$ structure stabilizer) additions suppressed pesting, while Al (C40 stabilizer) added alloys with pure C40 structure did[12]. However, a study on the effect of Al concentration on pesting in $MoSi_2$ showed that even as low as 5% (molar fraction) Al, i.e., single-phase $C11_b$, eliminated pesting at 500 ℃[13]. So, the structure of $MoSi_2$ is a less sensitive aspect for pesting than the alloying effect, even though the C40 structure might allow different solid solubilities than the $C11_b$ structure for the protective scale forming elements, e.g., Al and Cr. Therefore, the existence of small amounts of C40 phase detected by XRD in this study may play a secondary role on pesting.

Compared with monolithic $MoSi_2$ in this study, it is confirmed that a thin and more protective oxide scale is formed on the surface of powder metallurgy produced $(Mo,Cr)Si_2$ materials at 450 ℃. XRD and XPS analyses have shown that $SiO_2$ is the main constituent in the surface oxides. The mechanism of pesting resistance in the materials is not clear at this stage. Whether protective $Cr_2O_3$ is formed beneath the outermost surface or not at the pesting temperature, which is the objective of the material design, needs further examination.

Usually, both monolithic and $MoSi_2$-composites contain small amounts of $Mo_5Si_3$, resulting from excess Mo for manufacture reasons or oxidation of $MoSi_2$ during sintering, due to the strict stoichiometry of $MoSi_2$. However, it is pertinently noticed that $Cr_5Si_3$ grains with high Cr to Mo atomic ratio instead of $Mo_5Si_3$ phase is formed in the $MoSi_2$ matrix in this study. It is understandable for such a high Cr-content in $Mo_5Si_3$, as $Cr_5Si_3$-$Mo_5Si_3$ is an infinitive solid-solute system according to AGEEV[14]. As a result, the excess Cr in the $MoSi_2$ matrix is accommodated in the $(Cr,Mo)_5Si_3$ phase. It has been suggested that the existence of $Mo_5Si_3$ phase promotes accelerated oxidation due to high oxygen diffusion in $Mo_5Si_3$ phase[15]. Therefore, a mechanism of improved pesting resistance seen in this study for Cr-added $MoSi_2$ can be due to the formation of highly Cr-containing $Mo_5Si_3$.

## 4 Conclusions

Cr-alloyed $MoSi_2$ was compared with monolithic $MoSi_2$ with respect to oxidation at 450 ℃, which is in the so-called pest temperature range for $MoSi_2$, for 456 h. According to XRD, phases formed on Cr-alloyed $MoSi_2$ after exposure are $Cr_2(MoO_4)_3$, $MoO_3$, and cristobalite ($SiO_2$). Monolithic $MoSi_2$ forms $MoO_3$ and mainly amorphous $SiO_2$ as indicated by XRD and XPS. As indicated by XPS, the main oxidation product on the very top surface is $SiO_2$ for all three samples. All studied samples form a relatively loose, non-protective oxide but the oxide adherence improves with increasing Cr content. Also, the oxide thickness decreases with Cr-addition as indicated by the presence of bulk reflections in XRD for Cr-alloyed $MoSi_2$ as opposed to its monolithic counterpart.

## Acknowledgement

This study was partly sponsored by the Swedish Consortium for Materials Use in Energy Applications. Urban Jelvestam at Chalmers University of Technology is gratefully acknowledged for his help with the XPS experiments.

## References

[1] GRABKE H J, MEIER G H. Accelerated oxidation, internal oxidation, intergranular oxidation, and pesting of intermetallic compounds [J]. Oxid Met, 1995, 44: 147−176.

[2] YANAGIHARA K, PRZYBYLSKI K, MARUYAMA T. The role of microstructure on pesting during oxidation of $MoSi_2$ and $Mo(Si,Al)_2$ at 773 K [J]. Oxid Met, 1997, 47: 277−293.

[3] McKAMEY C G, TORTORELLI P F, DeVAN J H, CARMICHAEL

C A. A study of pest oxidation in polycrystalline $MoSi_2$ [J]. J Mater Res, 1992, 10: 2747−2755.

[4] PETROVIC J J, VASUDÉVAN A K. Key developments in high temperature structural materials [J]. Mater Sci Eng A, 1999, A261: 1−5.

[5] MEYER M K, THOM A J, AKINC M. Oxide scale formation and isothermal oxidation behavior of Mo-Si-B intermetallics at 600−1 000 ℃ [J]. Intermetallics, 1999, 7: 153−162.

[6] HARADA Y, MURATA Y, MORINAGA M. Solid solution softening and hardening inalloyed $MoSi_2$ [J]. Intermetallics, 1998, 6: 529−535.

[7] YI D, LAI Z, LI C, AKSELSEN O M, ULVENSOEN J H. Ternary alloying study of $MoSi_2$ [J]. Metall Mater Trans A, 1998, 29: 119−129.

[8] YANAGIHARA K, MARUYAMA T, NAGATA K. Effect of third elements on the pesting suppression of Mo-Si-X intermetallics (X=Al, Ta, Ti, Zr and Y) [J]. Intermetallics, 1996, 4: S133−S139.

[9] RAJ S V. A preliminary assessment of the properties of a chromium silicide alloy for aerospace applications [J]. Mater Sci Eng A, 1995, 192/193: 583−589.

[10] HARADA Y, MORINAGA M, SASO D, TAKATA M, SAKATA M. Refinement in crystal structure of $MoSi_2$ [J]. Intermetallics, 1998, 6: 523−527.

[11] UMAKOSHI Y, HIRANO T, SAKAGAMI T, YAMANE T. Yield stress and dislocation structure of $MoSi_2$ and $(Mo,Cr)Si_2$ single crystals [C]// High Temperature Aluminides and Intermetallics. TMS Warrendale, 1990: 111−132.

[12] STERGIOU A, TSAKIROPOULOS P. Oxidation studies on $MoSi_2$-X (X=Al, Ta, W) alloys [C]// Structural Intermetallics 1997. TMS Warrendale, 1997: 869−875.

[13] ARVANITIS A, WHITING M J, TSAKIROPOULOS P. A study of the oxidation behaviour of Mo-Si-Al intermetallic alloys at low, intermediate and high temperatures [C]// Structural Intermetallics 2001. TMS Warrendale, 2001: 561−570.

[14] AGEEV N V. Diagrammy sostoianiia metallicheskikh system [M]. Moscow: Viniti Press, 1964: 182.

[15] MESCHTER P J. Low-temperature oxidation of molybderum disilicide [J]. Metall Trans A, 1992, 23: 1763−1772.

**(Edited by LI Xiang-qun)**